Inclusion of Quantum Fluctuations in Wave Packet Dynamics*

Akira Ohnishi[a,b†] and Jørgen Randrup[b‡]
a. Department of Physics, Faculty of Science
Hokkaido University, Sapporo 060, Japan
b. Nuclear Science Division, Lawrence Berkeley Laboratory
University of California, Berkeley, CA 94720, USA
(14 April, 1996)

We discuss a method by which quantum fluctuations can be included in microscopic transport models based on wave packets that are not energy eigenstates. By including the next-to-leading order term in the cumulant expansion of the statistical weight, which corresponds to the wave packets having Poisson energy distributions, we obtain a much improved global description of the quantum statistical properties of the many-body system. In the case of atomic nuclei, exemplified by ^{12}C and ^{40}Ca, the standard liquid-drop results are reproduced at low temperatures and a phase transformation to a fragment gas occurs as the temperature is raised. The treatment can be extended to dynamical scenarios by means of a Langevin force emulating the transitions between the wave packets. The general form of the associated transport coefficients is derived and it is shown that the appropriate microcanonical equilibrium distribution is achieved in the course of the time evolution. Finally, invoking Fermi's golden rule, we derive specific expressions for the transport coefficients and verify that they satisfy the fluctuation-dissipation theorem.

1. INTRODUCTION

Microscopic simulations are employed in various fields of physics as tools for obtaining both of qualitative and quantitative insight. In these approaches, the many-body system is usually represented by a set of classical variables, even when it is basically quantal in character. For example, in molecular dynamics the many-body wave function is often represented as a (possibly antisymmetrized) product of parametrized single-particle wave packets, and the equations of motion for the parameters are then derived from a suitable variational principle. As a result, the quantal features of the system are not fully incorporated in the description. In particular, the system is no longer quantized and the quantum statistical properties are not properly accounted for. In effect, the statistical operator $\exp(-\beta\hat{H})$ is being replaced by the mean-field approximation to the statistical weight, $\exp(-\beta < \hat{H} >)$, although the wave packets are not energy eigenstates. The wave packet parameters then behave classically rather than quantally. This shortcoming is especially significant in scenarios where the statistical properties play a major role, such as complex processes, and, consequently, the quantitative utility of the results needs careful assessment.

This issue is especially relevant in the multifragmentation processes occurring in energetic collisions between atomic nuclei [1–3]. This phenomenon is of interest since it may provide information on the liquid-gas phase transition of nuclear matter that is expected because the nuclear forces resemble those of a Van der Waals gas. However, interpretation of the data must rely heavily on model simulations, due to the complexity of the collisions [4–10]. Since the constituent nucleons are fermions and the associated quantum statistical features persist to rather high temperatures, close to the transition temperature from the liquid to the gas phase, it may then be expected that the fragmentation pattern is influenced by the basic quantal nature of the nuclear system.

The outcome of complex processes, such as the fragment multiplicity distribution in nuclear collisions, is to a large degree governed by the statistical properties of the system, even if complete equilibrium is not reached. It is therefore important to understand to which extent the quantal statistical features are accounted for in the dynamical model employed. In our initial study [11], we examined the statistical equilibrium properties of Antisymmetrized Molecular Dynamics (*AMD*) [8] which describes the time-development of the Slater-determinant of single-particle Gaussian wave packets, and we considered especially non-interacting fermions in one dimension, either bound in a common harmonic potential or moving freely within an interval. Our principal conclusion was that the average excitation energy and the specific heat, considered as functions of the imposed temperature, generally behave in a classical manner when the canonical weight employed is consistent with the dynamics [11,12]. Furthermore, we found that the quantal statistical features could be recovered by taking account of the energy dispersion of each wave packet [11].

*Submitted to *Annals of Physics*, LBL-38596; HUPS-96-1
†E-mail: Ohnishi@nucl.phys.hokudai.ac.jp, Fax: +81-11-746-5444.
‡E-mail: Randrup@LBL.gov, Fax: +1-510-486-4794.

This result may at first appear somewhat surprising, since the underlying wave function is antisymmetric and the quantum statistical properties of the nuclear system to a large degree arises from the fermionic nature of the nucleons. Indeed, that work has generated some debate about the statistical character of wave packet dynamics, such as Fermionic Molecular Dynamics (*FMD*) [10] and *AMD*. In particular, Schnack and Feldmeier [13] (SF) and Ono and Horiuchi [14] (OH) have presented arguments in favor of the statistical properties of the wave packet systems being quantal rather than classical. One aim of the present paper is to elucidate this issue. We shall show that the energy dispersion of each wave packet plays a decisive role for the appearance of quantal statistical features and that it can be included in a natural manner by way of the cumulant expansion of the statistical weight. Moreover, the usual molecular dynamics leads to the classical statistical weight, $\exp(-\beta < \hat{H} >)$, while the quantal weight, $< \exp(-\beta \hat{H}) >$, can be well approximated by carrying the cumulant expansion to the next-to-leading order in β.

The modification of the statistical weight and the associated distortion of the internal structure of the wave packet naturally lead to a modification of the dynamics itself. In our preceding work [15], we have shown that the energy dispersion within each wave packet not only leads to the proper quantum statistical properties but also gives rise to a Langevin-type random force in the dynamics. In the field of nuclear physics, dynamical calculations with fluctuations have been applied to various dissipative phenomena, such as nuclear fission [16] and (idealized) nuclear collisions [17–19]. In the first case, the unretained microscopic degrees of freedom provide a heat bath that induces thermal fluctuations in the macroscopic degrees of freedom. In the latter case, the stochastic nature of the residual two-body collisions in the Boltzmann-Langevin model produces a statistical ensemble of possible dynamical histories for the one-body phase-space density. In contrast to those situations, the random force considered here has a purely quantal origin, as it arises from the energy dispersion of the individual wave packets, and it acts in addition to the statistical fluctuations induced by the residual scatterings.

The quantal Langevin force arises from the composite nature of each wave packet. This can be understood from the fact that an energy eigenstate, which is the observationally relevant entity, can be expanded in terms of the wave packets and therefore instantaneous transitions between those wave packets are possible. Furthermore, if the system is sufficiently complex to be ergodic, its time evolution will reflect the associated microcanonical ensemble. Since the wave packet has a finite energy dispersion, it may contribute to the phase volume even when its expectation value differs from the given energy. In the usual wave packet molecular dynamics, in which the equations of motion are obtained on the basis of the time-dependent variational principle, this kind of relaxation does occur because the expectation value of the Hamiltonian operator is conserved and so only the states lying on that hypersurface are dynamically accessible.

The principal aim of the present presentation is twofold. The first is to elucidate a microscopic theory that provides a satisfactory description of the quantum statistical properties of many-body systems such as nuclei, including the characteristic quantal behavior at low temperature and the transition from the quantum liquid to the fragment gas phase. We will show that this can be achieved by employing a simple approximate expression for the exact statistical weight, $\mathcal{W}_\beta =< \exp(-\beta \hat{H}) >$, which is derived by the standard cumulant expansion. At the same time, we illustrate the importance of the distortion of the wave packets caused by the canonical operator $\exp(-\beta \hat{H})$. This distortion modifies the expectation value associated with a given wave packet and is the key to resolving debate between our work and those of SF and OH.

The second aim is to use the insight gained from static scenarios to develop a corresponding dynamical theory in which transitions between states with different energy expectation values are possible and which relaxes towards the appropriate quantal microcanonical ensemble. We will show that this can be achieved by introducing a suitable Langevin force and employing Fermi's golden rule for specific expressions. The temperature can be defined without ambiguity and the Einstein relation between the drift and diffusion coefficients emerges naturally.

This paper is organized as follows. In section 2 we discuss the statistical properties of wave packet systems and show the importance of the energy fluctuation. In section 3 we then apply the proposed statistical model to finite nuclei, specifically ^{12}C and ^{40}Ca . The quantal microcanonical ensemble is then discussed in section 4 and we present the dynamical model with quantum fluctuations. Finally, section 5 summarizes our studies.

2. CANONICAL ENSEMBLE OF WAVE PACKETS

In order to set the framework for the discussion, we start by considering a canonical ensemble of parametrized many-body wave packets. The key quantity governing the statistical properties of a quantal many-body system is the associated partition function,

$$\mathcal{Z}(\beta) \equiv \mathrm{Tr}\ \mathrm{e}^{-\beta \hat{H}}\ , \tag{1}$$

where $\hat{H}$ is the many-body Hamiltonian operator and β is the inverse of the temperature of the canonical ensemble considered.

2.1. Wave packets

A central issue is how to calculate the statistical properties on the basis of the parametrized wave packets commonly employed in microscopic transport simulations. While our discussion and treatment apply rather generally, we shall work within the *AMD* framework, in order to allow concrete illustrations. As the basic wave functions we thus use Slater determinants of Gaussian wave packets, $(\boldsymbol{r}|\boldsymbol{z}) \sim \exp[-\nu(\boldsymbol{r} - \boldsymbol{z}/\sqrt{\nu})^2]$ [8]. The A-body wave packet $|\boldsymbol{Z})$ is then characterized by its complex centroid parameter vector, $\boldsymbol{Z} = (\boldsymbol{z}_1, \boldsymbol{z}_2, \ldots, \boldsymbol{z}_A)$, and the corresponding normalized wave packet is given by $|\boldsymbol{Z}> = |\boldsymbol{Z})/\sqrt{(\boldsymbol{Z}|\boldsymbol{Z})}$.

We assume that the wave packets provide a resolution of unity, as is the case in *AMD*. The anti-symmetrization operator is then represented as

$$\mathcal{A} = \int d\Gamma \; |\boldsymbol{Z}><\boldsymbol{Z}| \; . \tag{2}$$

The operator $\mathcal{A}$ projects onto the space of anti-symmetric wave functions, so it acts as unity within that space. In the *AMD* parametrization, the measure $d\Gamma$ is given by

$$d\Gamma(\boldsymbol{Z}) = \det \boldsymbol{C} \; d\boldsymbol{Z} d\bar{\boldsymbol{Z}} = \det \boldsymbol{C} \; \frac{d^{3A}\mathrm{Re}(\boldsymbol{Z}) \; d^{3A}\mathrm{Im}(\boldsymbol{Z})}{\pi^{3A}} \; . \tag{3}$$

In order to carry out the $6A$-dimensional integrals over $d\Gamma$, we have adopted a Metropolis sampling method, which guarantees that the computational effort is expended in proportion to the relative importance of the individual wave packets considered.

The action associated with a particular history $\boldsymbol{Z}(t)$ is given by $S[\boldsymbol{Z}(t)] = \int dt \; \mathcal{L}(t)$, where the Lagrangian is

$$\mathcal{L}(t) =< \boldsymbol{Z}|i\hbar\frac{\partial}{\partial t} - \hat{H}|\boldsymbol{Z} > \; . \tag{4}$$

The usual demand that the action be stationary then yields the equation of motion for the parameter vector $\boldsymbol{Z}$,

$$\frac{d\boldsymbol{Z}}{dt} = \frac{i}{\hbar}\boldsymbol{F} \; , \tag{5}$$

where the associated generalized force has been employed

$$\boldsymbol{F} = -\boldsymbol{C}^{-1} \cdot \frac{\partial \mathcal{H}}{\partial \bar{\boldsymbol{Z}}} \; . \tag{6}$$

The elements of the $A \times A$ coefficient matrix $\boldsymbol{C}$ are spatial tensors with complex elements,

$$C_{ij} = \frac{\partial^2}{\partial \bar{\boldsymbol{z}}_i \partial \boldsymbol{z}_j} \log \, (\boldsymbol{Z}|\boldsymbol{Z}) \; , \tag{7}$$

and $\mathcal{H}$ denotes the expectation value of the energy,

$$\mathcal{H} =< \boldsymbol{Z}|\hat{H}|\boldsymbol{Z} >= \frac{(\boldsymbol{Z}|\hat{H}|\boldsymbol{Z})}{(\boldsymbol{Z}|\boldsymbol{Z})} \; . \tag{8}$$

The equation of motion (5) is entirely classical and, if it can be brought onto canonical form, the partition function governing the statistical behavior of the wave packet parameter $\boldsymbol{Z}$ is given by the standard classical expression,

$$\mathcal{Z}^{\mathrm{Cl}}(\beta) = \int d\Gamma(\boldsymbol{Z}) \; \mathrm{e}^{-\beta\mathcal{H}(\boldsymbol{Z})} = \int d\Gamma(\boldsymbol{Z}) \; \mathcal{W}_\beta^{\mathrm{Cl}}(\boldsymbol{Z}) \; , \tag{9}$$

where $\mathcal{W}_\beta^{\mathrm{Cl}}(\boldsymbol{Z}) = \exp(-\beta\mathcal{H}(\boldsymbol{Z}))$ is the classical statistical weight of a given wave packet. Such a transformation has been shown to exist for the Gaussian wave packets employed in *AMD* [11], leading from the wave packet parameter $\boldsymbol{Z}$ to the phase-space variable $\boldsymbol{W} = \sqrt{\nu}\boldsymbol{q} + i\boldsymbol{p}/2\hbar\sqrt{\nu}$. The measure is then

$$d\Gamma(\boldsymbol{Z}) = d\boldsymbol{W} d\bar{\boldsymbol{W}} = \prod_{i=1}^{A} \frac{d\boldsymbol{p} d\boldsymbol{q}}{h^3} \; . \tag{10}$$

The above result (9) should be contrasted with the exact quantal partition function (1) which can also be expressed as an integral over the wave packet parameter space, since the wave packets employed resolve unity (see eq. (2)),

$$\mathcal{Z}(\beta) \equiv \mathrm{Tr} \; \mathrm{e}^{-\beta\hat{H}} = \int d\Gamma \; \mathcal{W}_\beta(\boldsymbol{Z}) \; . \tag{11}$$

However, the integrand is more complicated,

$$\mathcal{W}_\beta(\boldsymbol{Z}) \; \equiv < \boldsymbol{Z}| \; \mathrm{e}^{-\beta\hat{H}}|\boldsymbol{Z} > \; , \tag{12}$$

depending not merely on the expectation value $\mathcal{H} \equiv< \boldsymbol{Z}|\hat{H}|\boldsymbol{Z} >$ but also on the energy fluctuations inherent in the particular wave packet, as is further discussed below.

2.2. Statistical weight

It is a hard task to calculate the exact statistical weight, $\mathcal{W}_\beta(\boldsymbol{Z})$, since it contains A-body operators. It would in fact be equivalent to solving the dynamics exactly. It is therefore useful to develop an approximate treatment.

The main problem arises from the energy spread of the wave packets. Since a given wave packet is generally not an energy eigenstate, it has a distribution of energy eigenvalues, as is conveniently described by the associated strength function,

$$\rho_{_E}(\boldsymbol{Z}) \; \equiv < \boldsymbol{Z}|\delta(\hat{H} - E)|\boldsymbol{Z} > \neq \; \delta(\mathcal{H} - E) \; . \tag{13}$$

Consequently, the variance of the energy distribution is generally positive,

$$\sigma^2_{_E}(\boldsymbol{Z}) \equiv <\boldsymbol{Z}|\hat{H}^2|\boldsymbol{Z}> - <\boldsymbol{Z}|\hat{H}|\boldsymbol{Z}>^2 > 0 \ . \quad (14)$$

When these energy fluctuations are sufficiently small, the statistical weight can be evaluated in the "mean-field" or "static" approximation, yielding the classical result,

$$\mathcal{W}^{\rm Static}_\beta(\boldsymbol{Z}) = {\rm e}^{-\beta<\boldsymbol{Z}|\hat{H}|\boldsymbol{Z}>} = {\rm e}^{-\beta\mathcal{H}(\boldsymbol{Z})} = \mathcal{W}^{\rm Cl}_\beta(\boldsymbol{Z}) \ . \quad (15)$$

The statistical properties are then those of a classical system with the Hamiltonian function $\mathcal{H}(\boldsymbol{Z}) =< \boldsymbol{Z}|\hat{H}|\boldsymbol{Z} >$, *i.e.* the same as those exhibited by the wave packet parameter $\boldsymbol{Z}$, as discussed above. This correspondence remains true even for the *AMD* model, in which the fermionic nature of nucleons is incorporated by employing antisymmetrized wave packets [12,11].

We show below how to improve the calculation of the statistical properties when the energy fluctuations are significant. For this purpose, we first note that the statistical weight can be expressed as the norm of a wave function that evolves along the imaginary time direction,

$$\begin{aligned}\mathcal{W}_\beta(\boldsymbol{Z}) &\equiv <\boldsymbol{Z}|{\rm e}^{-\beta\hat{H}}|\boldsymbol{Z}> = <\boldsymbol{Z}|{\rm e}^{-\frac{1}{2}\beta\hat{H}}{\rm e}^{-\frac{1}{2}\beta\hat{H}}|\boldsymbol{Z}> \\ &= <\boldsymbol{Z}(\frac{\beta}{2})|\boldsymbol{Z}(\frac{\beta}{2})> , \end{aligned} \quad (16)$$

where the β dependent wave packet satisfies

$$\frac{\partial}{\partial\beta}|\boldsymbol{Z}(\beta)> = -\hat{H}|\boldsymbol{Z}(\beta)> , \quad (17)$$

and, consequently, changes its norm with β. The corresponding evolution equation for $\mathcal{W}_\beta$ is given by

$$\frac{\partial}{\partial\beta}\mathcal{W}_\beta(\boldsymbol{Z}) = -\mathcal{H}_\beta(\boldsymbol{Z})\mathcal{W}_\beta(\boldsymbol{Z}) , \quad (18)$$

with the β dependent energy expectation given by

$$\mathcal{H}_\beta(\boldsymbol{Z}) \equiv \frac{<\boldsymbol{Z}(\beta/2)|\hat{H}|\boldsymbol{Z}(\beta/2)>}{<\boldsymbol{Z}(\beta/2)|\boldsymbol{Z}(\beta/2)>} . \quad (19)$$

The formal solution to eq. (18) is

$$\mathcal{W}_\beta(\boldsymbol{Z}) = \exp\left[-\int_0^\beta d\beta' \ \mathcal{H}_{\beta'} \right] . \quad (20)$$

This expression for the statistical weight is exact, and when the quantal state $|\boldsymbol{Z}>$ is an energy eigenstate, eq. (20) is the usual statistical weight $\mathcal{W}_\beta = \exp(-\beta E)$, where E is the associated eigenvalue. The difference between (15) and (20) comes from the fact that the given state $|\boldsymbol{Z}>$ is not an energy eigenstate so its energy distribution must be taken into account.

The quantal weight (20) can be calculated once we know the β dependence of the expectation value of the Hamiltonian operator, $\mathcal{H}_\beta(\boldsymbol{Z})$. Generally, $\mathcal{H}_\beta(\boldsymbol{Z})$ decreases as the temperature is reduced, since the distortion of the wave packet caused by the canonical factor $\exp(-\beta E)$ is then more effective. This feature can also be brought out by a direct differentiation of $\mathcal{H}_\beta$,

$$\begin{aligned}\frac{\partial}{\partial\beta}\mathcal{H}_\beta(\boldsymbol{Z}) &= -\left(\frac{<\boldsymbol{Z}(\beta/2)|\hat{H}^2|\boldsymbol{Z}(\beta/2)>}{<\boldsymbol{Z}(\beta/2)|\boldsymbol{Z}(\beta/2)>} - \mathcal{H}^2_\beta \right) \\ &= -\sigma^2_{_E}(\boldsymbol{Z}(\beta/2)) \le 0 . \end{aligned} \quad (21)$$

Furthermore, if the given state $|\boldsymbol{Z}>$ is not orthogonal to the ground state, as is always true for the generalized coherent states usually employed, then $\mathcal{H}_\beta(\boldsymbol{Z})$ converges to the ground state energy $E_{\rm gs}$ as $\beta \to \infty$.

In order to develop a suitable approximation to $\mathcal{W}_\beta(\boldsymbol{Z})$, we perform a first-order logarithmic expansion of $\mathcal{H}_\beta(\boldsymbol{Z})$,

$$\log\mathcal{H}_\beta(\boldsymbol{Z}) \approx \log\mathcal{H}(\boldsymbol{Z}) + \beta\frac{\partial}{\partial\beta}\log\mathcal{H}_\beta(\boldsymbol{Z})|_{\beta=0} , \quad (22)$$

and find

$$\mathcal{H}_\beta(\boldsymbol{Z}) \approx \mathcal{H}(\boldsymbol{Z}) \ {\rm e}^{-\beta D(\boldsymbol{Z})} . \quad (23)$$

Here the effective level spacing D is equal to the relative energy variance of the state considered,

$$D(\boldsymbol{Z}) \equiv -\frac{\partial}{\partial\beta}\log\mathcal{H}_\beta(\boldsymbol{Z})\Big|_{\beta=0} = \sigma^2_{_E}(\boldsymbol{Z})/\mathcal{H}(\boldsymbol{Z}) . \quad (24)$$

Eq. (20) then yields the corresponding statistical weight,

$$\mathcal{W}_\beta(\boldsymbol{Z}) \approx \exp\left[-\frac{\mathcal{H}}{D}\left(1-{\rm e}^{-\beta D}\right) \right] , \quad (25)$$

where the ground-state energy has been subtracted from the Hamiltonian, $\mathcal{H}(\boldsymbol{Z}_{\rm gs}) = 0$.

In order to elucidate this approximation, we consider a harmonic oscillator with the level spacing Δ and employ wave packets of coherent form, $|\boldsymbol{Z}) = \exp(-\boldsymbol{Z}a^\dagger)|0>$. The normalized state is then

$$|\boldsymbol{Z}> = {\rm e}^{-\frac{1}{2}\bar{\boldsymbol{Z}}\boldsymbol{Z}} \sum_n \frac{\boldsymbol{Z}^n}{\sqrt{n!}} |n> , \quad (26)$$

and its mean energy is $\mathcal{H}(\boldsymbol{Z}) = \bar{\boldsymbol{Z}}\boldsymbol{Z}\Delta$. Moreover, the corresponding spectral distribution is of Poisson form,

$$\rho_n(\boldsymbol{Z}) = \frac{1}{n!}\left(\frac{\mathcal{H}}{\Delta}\right)^n {\rm e}^{-\mathcal{H}/\Delta} = \frac{1}{n!}\left(\bar{\boldsymbol{Z}}\boldsymbol{Z}\right)^n {\rm e}^{-\bar{\boldsymbol{Z}}\boldsymbol{Z}} . \quad (27)$$

The β evolution of the wave packet $|\boldsymbol{Z}>$ is easily obtained,

$$|\boldsymbol{Z}(\beta/2)> = {\rm e}^{-\frac{1}{2}\bar{\boldsymbol{Z}}\boldsymbol{Z}} \sum_n \frac{\boldsymbol{Z}^n}{\sqrt{n!}} {\rm e}^{-\frac{1}{2}n\beta\Delta} |n> , \quad (28)$$

so, according to eq. (16), the statistical weight then becomes

$$\mathcal{W}_\beta(\boldsymbol{Z}) = \mathrm{e}^{-\bar{\boldsymbol{Z}}\boldsymbol{Z}} \sum_n \frac{1}{n!} (\bar{\boldsymbol{Z}}\boldsymbol{Z})^n \mathrm{e}^{-n\beta\Delta}$$
$$= \exp\left[-\bar{\boldsymbol{Z}}\boldsymbol{Z}(1-\mathrm{e}^{-\beta\Delta})\right] . \quad (29)$$

The β dependence of $\mathcal{H}$ can then be obtained by differentiation,

$$\mathcal{H}_\beta(\boldsymbol{Z}) = -\frac{\partial}{\partial\beta}\log\mathcal{W}_\beta(\boldsymbol{Z}) = \bar{\boldsymbol{Z}}\boldsymbol{Z}\Delta\ \mathrm{e}^{-\beta\Delta}$$
$$= \mathcal{H}(\boldsymbol{Z})\ \mathrm{e}^{-\beta\Delta} . \quad (30)$$

Thus the Hamiltonian $\mathcal{H}_\beta(\boldsymbol{Z})$ exhibits a pure exponential damping. It then follows that the associated effective level spacing, $D \equiv -\partial\log\mathcal{H}/\partial\beta$, is simply equal to the level spacing of the oscillator, Δ. Furthermore, we see that the expression (25) for the statistical weight in fact agrees with the exact result (29), with $\mathcal{H}/D$ representing the mean number of quanta in the state, $< n >= \mathcal{H}/\Delta = \bar{\boldsymbol{Z}}\boldsymbol{Z}$.

The expressions ((23) and (24)) are those already used in our previous work [11]. It was shown there that they yield the proper statistical properties, in certain exactly soluble cases. We also note that the statistical weight (25) can be obtained from the general cumulant expansion,

$$\log\mathcal{W}_\beta(\boldsymbol{Z}) = -\beta\mathcal{H}(\boldsymbol{Z}) + \frac{1}{2}\beta^2\mathcal{H}(\boldsymbol{Z})D(\boldsymbol{Z}) + \cdots$$
$$= -\beta\mathcal{H}(\boldsymbol{Z}) + \frac{1}{2}\beta^2\sigma_{_E}^2(\boldsymbol{Z}) + \cdots . \quad (31)$$

The lowest-order term is recognized as the static result, eq. (15), while the inclusion of the next term yields the present refined treatment, eq. (25). By carrying the cumulant expansion to higher order, increasingly refined approximations can thus be developed, if called for. The approximation adopted here is exact in the case of distinguishable particles in a harmonic oscillator potential. Therefore we refer to this treatment as the *Harmonic Approximation*.

2.3. Expectation values

The effect of the canonical operator $\exp(-\beta\hat{H})$ on a wave packet is two-fold. The most obvious effect is the assignment of a statistical weight for the wave packet as a whole, $\mathcal{W}_\beta(\boldsymbol{Z})$, as described above. However, since each energy component is weighted differently (namely according to its eigenenergy), the statistical operator also introduces a distortion of the internal structure of the wave packet. This latter effect generally modifies the expectation value of quantal operators and, as a consequence, the evaluation of thermal expectation values is less straightforward than one might at first have thought.

In general the canonical expectation value of a quantal operator $\hat{O}$ is given by

$$\prec \mathcal{O} \succ_\beta \equiv \frac{1}{\mathcal{Z}(\beta)}\mathrm{Tr}\left[\hat{O}\ \mathrm{e}^{-\beta\hat{H}}\right] . \quad (32)$$

Using the resolution in terms of the wave packets, eq. (2), the above expectation value can be written on standard form as a weighted average,

$$\prec \mathcal{O} \succ_\beta = \frac{1}{\mathcal{Z}(\beta)}\int d\Gamma(\boldsymbol{Z})\ \mathcal{O}_\beta(\boldsymbol{Z})\ \mathcal{W}_\beta(\boldsymbol{Z}) , \quad (33)$$

where the value of the observable associated with a given wave packet $|\boldsymbol{Z}>$ is the expectation value of $\mathcal{O}$ in the *distorted* state $|\boldsymbol{Z}(\beta/2)>$,

$$\mathcal{O}_\beta(\boldsymbol{Z}) \equiv < \hat{O} >_\beta \equiv \frac{<\boldsymbol{Z}|\mathrm{e}^{-\beta\hat{H}/2}\hat{O}\mathrm{e}^{-\beta\hat{H}/2}|\boldsymbol{Z}>}{<\boldsymbol{Z}|\ \mathrm{e}^{-\beta\hat{H}}|\boldsymbol{Z}>}$$
$$= \frac{<\boldsymbol{Z}(\beta/2)|\hat{O}|\boldsymbol{Z}(\beta/2)>}{<\boldsymbol{Z}(\beta/2)|\boldsymbol{Z}(\beta/2)>} . \quad (34)$$

When the temperature is sufficiently high in comparison with the effective level spacing, $T \gg D = \sigma_{_E}^2/\mathcal{H}$, the distortion is very small and we have,

$$\prec \mathcal{O} \succ_\beta^{\mathrm{Cl}} = \frac{1}{\mathcal{Z}(\beta)}\int d\Gamma(\boldsymbol{Z})\ <\boldsymbol{Z}|\hat{O}|\boldsymbol{Z}>\mathcal{W}_\beta(\boldsymbol{Z}) . \quad (35)$$

It is relatively easy to exhibit the effect of the thermal distortion of the wave packets when the temperature is high. An expansion of eq. (34) shows that the leading correction to the classical result (35) is proportional to the quantal correlation between the observable $\hat{O}$ and the Hamiltonian $\hat{H}$,

$$\mathcal{O}_\beta(\boldsymbol{Z}) = \mathcal{O}(\boldsymbol{Z}) - \beta\left[<\boldsymbol{Z}|\frac{1}{2}\{\hat{O},\hat{H}\}|\boldsymbol{Z}> - \mathcal{O}(\boldsymbol{Z})\ \mathcal{H}(\boldsymbol{Z})\right]$$
$$+ \cdots , \quad (36)$$

where $\{\cdot,\cdot\}$ denotes the anti-commutator. Thus, the expectation value of $\hat{O}$ in the thermally distorted state decreases if the correlation is positive and conversely.

However, in cases of practical interest the thermal distortion is not negligible and must be taken into account in order to obtain quantitatively useful results [11]. The effect is well illustrated by the behavior of the mean energy of the thermal ensemble of wave packets. Assuming that $\mathcal{H}_\beta(\boldsymbol{Z})$ exhibits a simple exponential evolution, as in eq. (23), the mean energy can be expressed as

$$\prec \mathcal{H} \succ_\beta = \frac{1}{\mathcal{Z}(\beta)}\int d\Gamma(\boldsymbol{Z})\ \mathcal{H}(\boldsymbol{Z})\ \mathrm{e}^{-\beta D}\mathcal{W}_\beta(\boldsymbol{Z}) . \quad (37)$$

The distortion factor $\mathrm{e}^{-\beta D}$ suppresses the contribution from a given wave packet (as it should, since it is positively correlated with itself), and it ensures that the characteristic quantal behavior, $E^* \propto \mathrm{e}^{-\beta D}$, emerges at low temperature, $T \ll D$.

2.4. Discussion and illustrations

In our initial work, we pointed out that the standard *AMD* model exhibits classical statistical properties and suggested that the situation be remedied by including of the energy fluctuation of each wave packet [11]. That work has generated some debate about the nature of the statistical properties of wave packet molecular dynamics, such as FMD and AMD. In particular, Schnack and Feldmeier [13] (SF) and Ono and Horiuchi [14] (OH) have made the counterclaim that the statistical properties of the wave packet systems are quantal rather than classical. Hoping to elucidate the issue, we now discuss and illustrate the situation in some detail.

In their analyses, both SF and OH focus on the occupation probability for the single-particle levels in a harmonic-oscillator potential. Specifically, they consider the quantity

$$P_n(\beta) \equiv \frac{1}{\mathcal{Z}(\beta)} \int d\Gamma(\boldsymbol{Z}) \ < \boldsymbol{Z}|\hat{O}_n|\boldsymbol{Z} > \mathcal{W}_\beta(\boldsymbol{Z}) \ , \quad (38)$$

where $\hat{O}_n = a_n^\dagger a_n$ is the one-body operator counting the number of particles in the level n. In the work by SF, the integral over $d\Gamma$ is carried out through the time-evolution of FMD wave functions in the harmonic oscillator potential with a perturbative residual interaction; they have also studied the thermalization between two oscillators with different frequencies. The work by OH employs the same wave packets and measure as our original work [11], and they have also studied actual nuclear systems by using the evaporated nucleons as a thermometer. The results of these studies of the harmonic oscillator can be summarized as follows. When the initial energy (SF) or the temperature (OH) is chosen so as to reproduce the mean energy of the corresponding quantal canonical ensemble, then the quantity P_n emerges as being very similar to the occupation probability of the quantal canonical ensemble.

This result is not unexpected, since both of *FMD* and *AMD* are based on totally anti-symmetrized wave functions and therefore take account of the Fermi statistics governing the individual particles. Moreover, the relation between temperature and energy in the ensembles employed by SF and OH is by construction the quantal one. However, this type of analysis does not address the key issue, namely the many-body properties of the system. In order to clarify the situation, we discuss the following three separate issues:

1. *Statistical weight.* The statistical weight $\mathcal{W}_\beta$ employed in the integration over parameter space can be calculated either quantally (Q) or classically (Cl),

   - Quantal statistical weight:

   $$\mathcal{W}_\beta^{\rm Q} = < \boldsymbol{Z}| \exp(-\beta \hat{H})|\boldsymbol{Z} > \ . \quad (39)$$

   - Classical statistical weight:

   $$\mathcal{W}_\beta^{\rm Cl} = \exp\left(-\beta \mathcal{H}\right) \ . \quad (40)$$

2. *Expectation value.* The value of the observable associated with a given wave packet can be calculated with either the thermally distorted states (D) or the undistorted states (U),

   - Observation with distorted states:

   $$\mathcal{O}_\beta^{\rm D}(\boldsymbol{Z}) = \frac{< \boldsymbol{Z}|{\rm e}^{-\beta\hat{H}/2}\hat{O}{\rm e}^{-\beta\hat{H}/2}|\boldsymbol{Z} >}{< \boldsymbol{Z}|{\rm e}^{-\beta\hat{H}}|\boldsymbol{Z} >} \equiv \mathcal{O}_\beta(\boldsymbol{Z}) \quad (41)$$

   - Observation with undistorted states:

   $$\mathcal{O}_\beta^{\rm U} = < \boldsymbol{Z}|\hat{O}|\boldsymbol{Z} > \equiv \mathcal{O}(\boldsymbol{Z}) \quad (42)$$

3. *Temperature.* The temperature can be either taken as the specified one (T) or readjusted so the expectation value of the energy is matched exactly (T'),

   - T: The given temperature $T = 1/\beta$ is the one used for the statistical weight and the observation.
   - T': The given temperature T is regarded as spurious and is replaced by T' which is obtained by demanding that the mean energy of the system match the exact value.

The exact calculation discussed in the previous section then corresponds to the option [Q-D-T], whereas the calculation by OH corresponds to [Cl-U-T']. Although SF perform the ensemble sampling by means of the time evolution, their residual interaction ensures ergodicity and the treatment by SF is then be essentially the same as that by OH.

To illustrate the effect of the different treatments, we consider four fermions in a harmonic oscillator and calculate the occupation probability of each single particle level, for various temperatures. Figure 1 shows the results based on either distorted (D) or undistorted (U) wave packets and employing the options [Q-T], [Cl-T], and [Cl-T'] in each case. The quantal statistical weights were calculated in the harmonic approximation, and the quantal observation is carried out by assuming the β evolution of $\boldsymbol{z}_i$ to be $\boldsymbol{z}_i(\beta/2) = \boldsymbol{z}_i(0)\exp(-\beta\hbar\omega/2)$.

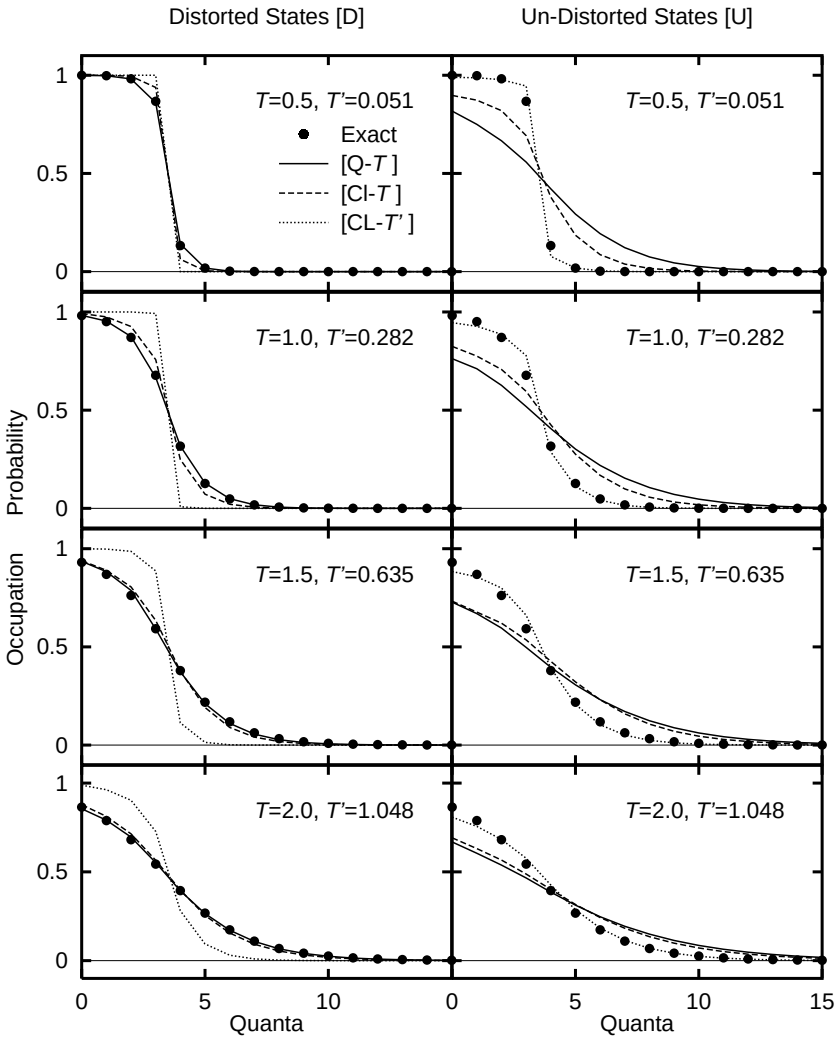

FIG. 1. Occupation probability in a harmonic oscillator.

The occupation probability for four identical fermions in a harmonic potential calculated with either distorted states (D: left) or undistorted states (U: right) for the observation of the occupation number and employing the options [Q-T], [Cl-T], and [Cl-T'] in each case. About 10^4 states were sampled for each temperature by means of the Metropolis method. The exact quantal results are shown by the solid dots.

Comparison with the exact result (solid dots) shows that both [Q-D-T] and [Cl-U-T'] reproduce the exact results very well, which is in accordance with the reports by SF and OH. Even though the latter treatment is not formally correct, this agreement is not unexpected, as we shall now discuss. The key to achieving a correspondence between the two treatments is to regard the distorted state $|\boldsymbol{Z}(\beta/2)>$ as the state $|\boldsymbol{Z}'>$ sampled by SF and OH. Then, in the harmonic approximation where $\mathcal{H}_\beta = \mathcal{H}\exp(-\beta D)$, the quantal statistical weight $\mathcal{W}_\beta^{\rm Q}$ can be rewritten in terms of a modified inverse temperature β' and the expectation value with respect to $|\boldsymbol{Z}'>$,

$$\begin{aligned}\log \mathcal{W}_\beta^{\rm Q}(\boldsymbol{Z}) &\equiv -\frac{\mathcal{H}(\boldsymbol{Z})}{D}\left(1-{\rm e}^{-\beta D}\right)\\ &= -\frac{\mathcal{H}(\boldsymbol{Z}')\ {\rm e}^{\beta D}}{D}\left(1-{\rm e}^{-\beta D}\right)\\ &= -\beta'\ \mathcal{H}(\boldsymbol{Z}') \ \equiv\ \log \mathcal{W}_{\beta'}^{\rm Cl}(\boldsymbol{Z}')\ , \end{aligned} \tag{43}$$

where the modified temperature is determined by

$$\beta' = \frac{{\rm e}^{\beta D}-1}{D} = \beta(1+\frac{1}{2}\beta D+\ldots)\ . \tag{44}$$

Consequently, the quantal partition function can be expressed in terms of the classical statistical weight for the distorted state,

$$\mathcal{Z}^{\rm Q}(\beta) \equiv \int d\Gamma(\boldsymbol{Z})\ \mathcal{W}^{\rm Q}_{\beta}(\boldsymbol{Z}) = \int J\ d\Gamma(\boldsymbol{Z}')\ \mathcal{W}^{\rm Cl}_{\beta'}(\boldsymbol{Z}')\ , \tag{45}$$

where J is the Jacobian associated with the transformation from $\boldsymbol{Z}$ to $\boldsymbol{Z}'$,

$$J \ \equiv\ \left| \begin{array}{cc} \boldsymbol{W} & \bar{\boldsymbol{W}} \\ \boldsymbol{W}' & \bar{\boldsymbol{W}}' \end{array} \right| \ =\ \frac{\det \boldsymbol{C}}{\det \boldsymbol{C}'} \left| \begin{array}{cc} \boldsymbol{Z} & \bar{\boldsymbol{Z}} \\ \boldsymbol{Z}' & \bar{\boldsymbol{Z}}' \end{array} \right| \ . \tag{46}$$

Comparing the above reformulation (45) with the classical partition function,

$$\mathcal{Z}^{\rm Cl}(\beta') = \int d\Gamma(\boldsymbol{Z}')\ \mathcal{W}^{\rm Cl}_{\beta'}(\boldsymbol{Z}')\ , \tag{47}$$

we see that if the Jacobian J is independent of $\boldsymbol{Z}$ then the two partition functions are proportional,

$$\mathcal{Z}^{\rm Q}(\beta) = J\ \mathcal{Z}^{\rm Cl}(\beta')\ , \tag{48}$$

In addition, the expectation value $\mathcal{O}_{\beta}(\boldsymbol{Z})$ is then the same as $< \boldsymbol{Z}'|\hat{O}|\boldsymbol{Z}' >$ by definition. Consequently, the thermal averages of the observable $\hat{O}$ are also equal,

$$\begin{aligned} \prec \mathcal{O} \succ^{\rm Q}_{\beta} \ &\equiv \frac{1}{\mathcal{Z}^{\rm Q}(\beta)} \int d\Gamma(\boldsymbol{Z})\ \mathcal{O}^{\rm Q}_{\beta}(\boldsymbol{Z})\ \mathcal{W}^{\rm Q}_{\beta}(\boldsymbol{Z}) \\ &= \frac{1}{J\ \mathcal{Z}^{\rm Cl}(\beta)}\ J \int d\Gamma(\boldsymbol{Z}')\ \mathcal{O}^{\rm Cl}_{\beta'}\ \mathcal{W}^{\rm Cl}_{\beta'}(\boldsymbol{Z}') \\ &= \prec \mathcal{O} \succ^{\rm Cl}_{\beta'}\ . \end{aligned} \tag{49}$$

This result brings out very clearly how it is possible, for each given temperature T, to introduce a modified temperature T' so that the quantal result is reproduced.

However, this kind of treatment leads to inconsistent thermodynamics. The mean energy $\prec \mathcal{H} \succ$ should be given by $-\partial \log \mathcal{Z}/\partial\beta$, and that is indeed the case in the approximate quantal treatment of ref. [11]. But the modified treatment in [Cl-U-T'] yields the mean energy

$$\prec \mathcal{H} \succ^{\rm Cl}_{\beta} = \ \frac{1}{\mathcal{Z}^{\rm Cl}(\beta')} \int d\Gamma(\boldsymbol{Z}')\ \mathcal{H}(\boldsymbol{Z}')\ \mathcal{W}^{\rm Cl}_{\beta'}(\boldsymbol{Z}')\ , \tag{50}$$

while a differentiation of the partition function (45) leads to

$$-\ \frac{\partial}{\partial\beta} \log \mathcal{Z}^{\rm Cl}_{\beta} = \frac{1}{\mathcal{Z}^{\rm Cl}(\beta)} \int d\Gamma(\boldsymbol{Z}')\ \mathcal{H}(\boldsymbol{Z}')\ {\rm e}^{\beta D}\ \mathcal{W}^{\rm Cl}_{\beta'}(\boldsymbol{Z}')\ , \tag{51}$$

which contains the additional factor $d\beta'/d\beta = \exp(\beta D)$. Therefore, the modification of the temperature parameter renders the thermodynamics inconsistent.

A further difference between the two treatments is the partition function itself. The classical partition function $\mathcal{Z}^{\rm Cl}$ deviates from the quantal partition function $\mathcal{Z}^{\rm Q}$ by the Jacobian factor J. If the determinant ratio $\det \boldsymbol{C}/\det \boldsymbol{C}$ is ignored, we have $J \simeq \exp(-A\beta D)$. This ideal situation is realized in the case of A distinguishable particles in a harmonic oscillator potential, where the level spacing $D = \hbar\omega$ is a constant. Furthermore, the Jacobian J is independent of $\boldsymbol{Z}$ but still depends on β, of course. The partition functions $\mathcal{Z}^{\rm Q}$ and $\mathcal{Z}^{\rm Cl}$ are shown in fig. 2. While the quantal partition function approaches unity when $T \to 0$, the classical partition function tends to zero. This occurs because the phase space for $\boldsymbol{Z}'$ is drastically reduced relative to the original phase space of $\boldsymbol{Z}$ when the temperature is smaller than the level spacing, as already discussed. The fact that the phase space, and hence also the statistical fluctuations, are too small in the ensembles employed by SF and OH may present a practically important shortcoming of those treatments, since the partition function is the key quantity governing the fragment size distribution in actual nuclear collision processes.

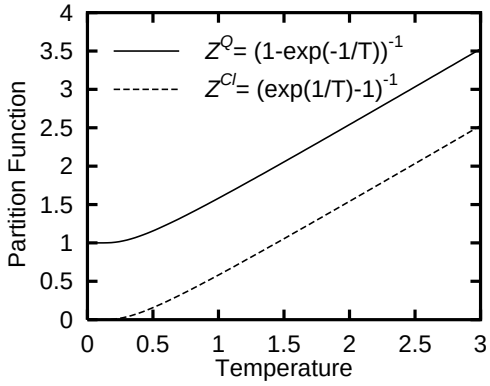

FIG. 2. Partition function for a harmonic oscillator. The partition function for A distinguishable particles in a harmonic potential, calculated either quantally (Q: solid curve) or classically (Cl: dashed curve). The temperature is expressed in units of the oscillator spacing $D = \hbar\omega$.

3. STATISTICAL PROPERTIES OF FINITE NUCLEI

In the previous section, we employed a few simple soluble cases to illustrate the general treatment. We now turn to more realistic scenarios and consider the statistical properties of finite nuclei.

As we have seen, we need to determine the β evolution of the wave packet. In the harmonic approximation, this is equivalent to calculating the energy dispersion $\sigma^2_{_E}(\boldsymbol{Z})$ of the wave packet, since level spacing $D = \sigma^2_{_E}/\mathcal{H}$ is the

key quantity determining the statistical weight. More generally, the equations of motion (EOM) for the wave packet parameters $\boldsymbol{Z}$ can be employed for this task by replacing the real time t by the imaginary time $-i\hbar\beta$. In the *AMD* model,

$$\frac{\partial \boldsymbol{Z}}{\partial t} = \frac{i}{\hbar}\boldsymbol{F} \qquad \overset{t\to -i\hbar\beta}{\to} \qquad \frac{\partial \boldsymbol{Z}}{\partial \beta} = \boldsymbol{F}\ . \tag{52}$$

The first equation governs the usual time development, while the second one can be used for the estimation of the statistical weight. It may be noted that the second equation is usually employed for the construction of the ground-state nuclei, such as those used as initial conditions in nucleus-nucleus collisions, since it effectively cools the system down. It is therefore refered to as the "cooling" equation [8].

In the present work, we have adopted eq. (25) as the statistical weight,

$$\mathcal{W}_\beta(\boldsymbol{Z}) = \exp\left[-\frac{\mathcal{H}}{D}\left(1-\mathrm{e}^{-\beta D}\right)\right]\ , \tag{53}$$

and the effective level spacing associated with a given wave packet $|\boldsymbol{Z}>$ is calculated by the *AMD* cooling equation,

$$\begin{aligned} D(\boldsymbol{Z}) &= -\frac{\partial}{\partial\beta}\log\mathcal{H}_\beta\Big|_{\beta=0} \\ &= -\frac{1}{2\mathcal{H}}\left[\frac{\partial\mathcal{H}}{\partial\boldsymbol{Z}}\frac{\partial\boldsymbol{Z}}{\partial\beta} + \frac{\partial\mathcal{H}}{\partial\bar{\boldsymbol{Z}}}\frac{\partial\bar{\boldsymbol{Z}}}{\partial\beta}\right] = \bar{\boldsymbol{F}}\cdot\frac{\boldsymbol{C}}{\mathcal{H}}\cdot\boldsymbol{F}\ . \end{aligned} \tag{54}$$

Working in the harmonic approximation where $\mathcal{H}_\beta = \mathcal{H}\exp(-\beta D)$, we wish to calculate the temperature dependence of the mean energy $\prec \mathcal{H} \succ_\beta$ and the specific heat,

$$\begin{aligned} C_V(\beta) &\equiv -\beta^2\frac{\partial^2}{\partial\beta^2}\log\boldsymbol{Z}(\beta) \\ &= \beta^2\left[\prec < \hat{H}^2 >_\beta \succ_\beta - \prec \mathcal{H} \succ^2\right]\ , \end{aligned} \tag{55}$$

where the expectation value of $\hat{H}^2$ is given by

$$< \hat{H}^2 >_\beta = D\ \mathcal{H}(\boldsymbol{Z})\ \mathrm{e}^{-\beta D} = \sigma_E^2(\boldsymbol{Z})\ \mathrm{e}^{-\beta D}\ . \tag{56}$$

The harmonic approximation demands that D is constant along the β evolution described by the cooling equation. This is not strictly true for real nuclei, since the energy surface is not exactly quadratic. However, at low excitations a quadratic behavior holds approximately since the first derivative of $\mathcal{H}$ vanishes in the ground state. Moreover, at high temperatures where β expansion is valid, the quantum fluctuaton effects are well described by the cumulant expansion and the harmonic approximation is then reliable in this regime as well. Therefore we expect the harmonic approximation to provide a reasonable starting point.

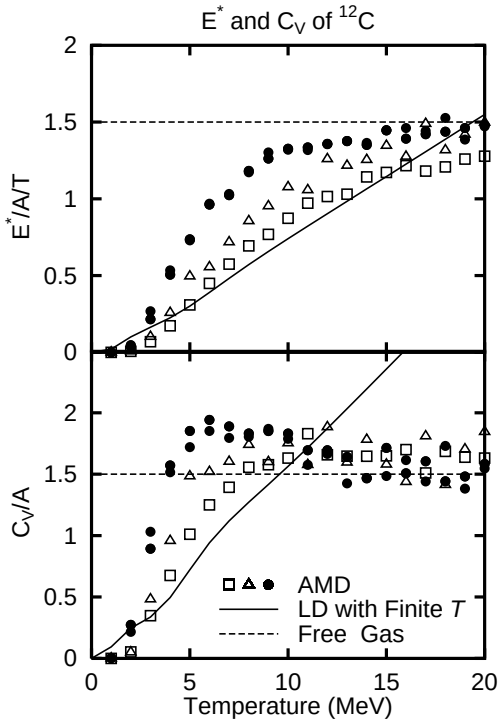

FIG. 3. Excitation energy and specific heat of ^{12}C.

The mean excitation energy per nucleon E^*/A divided by the temperature T (top) and the specific heat per particle C_V/A (bottom) for a canonical ensemble of ^{12}C nuclei calculated with the *AMD* model, as a function of the temperature T. Squares, triangles and circles show the results obtained with various values of the radius constant, $r_0 = 1.2, 1.5, 2.0$ fm, respectively. Also shown are the results for a free classical gas (dashed lines) and a nuclear liquid drop model (solid curves) in which the excitation spectrum contains the known low-energy levels plus a Fermi-Dirac gas of quasi-particles with a suitably modified level-density parameter, $a = A/(8\ \mathrm{MeV})(1-0.8/A^{1/3})$ [22]. The marks represent results with three different freeze-out volumes, $V = 4\pi R^3/3, R = r_0 A^{1/3}$, r_0=1.2, 1.5, 2.0 fm. The sample size for each scenario is 5×10^4. In order to give an impression of the sampling error, the results of two different ensembles are shown for $r_0 = 2.0$ fm.

Using the above framework, we have studied the statistical properties of ^{12}C and ^{40}Ca with the *AMD* model. The effective nuclear interaction used is Volkov No. 1 [20] and the width parameter ν and the Majorana mixture are chosen so as to fit the binding energy and the *r.m.s.* radius. The phase space integral are evaluated by means of a Metropolis sampling method.

Figure 3 shows the excitation energy E^* and the specific heat C_V of ^{12}C as a function of the temperature. For convenience, the excitation energy has been divided

by the temperature (the free value is then a constant (= 3/2)). For comparison, we also show E^* and C_V for free classical particles (dashed line) and for a finite-temperature liquid drop model that includes known low-energy nuclear levels augmented by a Fermi-Dirac gas (solid curve).

The calculated results exhibit the expected behavior: At low temperature the excitation energy behaves quadratically, $E^*/A \approx aT^2$, and as the temperature increases it approaches its free value, $E^*_{\rm free} = 3T/2$. This behavior is consistent with the transition from the liquid phase (or quantal phase) to the gas phase (or classical phase). The same features appear for the specific heat: It grows approximately linearly at low temperatures, $C_V/A \approx 2aT$, and then approaches its free value, $C_V^{\rm free}/A = 3/2$. In addition, the low-temperature results obtained for normal density, $r_0 = 1.2$ fm, are very close to those of the standard liquid drop model. These results are very satisfactory, since they yield a good description of the statistical properties of finite nucleus over the entire range of temperatures.

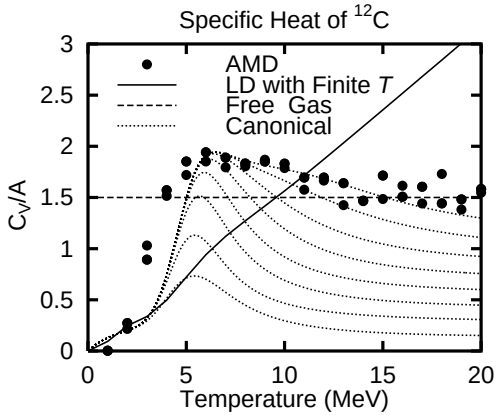

FIG. 4. Specific heat and fragmentation of ^{12}C.

The specific heat per nucleon calculated with *AMD* (solid dots) and with the canonical multifragmentation model described in the text admitting a maximum of N fragments, with N=2–9 (short dashes). The radius constant was taken as $r_0 = 2.0$ fm, corresponding to a freeze-out density equal to about 20% of normal. Also shown are the results for the liquid drop model (solid curve) and the free nucleon gas (long dashes).

It is interesting to study the volume dependence of these quantities, since the freeze-out volume is the most important parameter in the statistical models of multifragmentation, *i.e.*, it determines the ratio between binary and multifragment decays [21]. The qualitative behavior (the transition from the liquid-like phase to the gas-like phase) does not change with volume, but it becomes easier to excite the system when the volume grows larger. This is because the excitation of intrinsic modes in a single nucleus is being overwhelmed by the agitation of multi-fragment configurations. In addition, there appears a region in which the specific heat exceeds its free value of 3/2, reflecting the rapid activation of many degrees of freedom that were effectively frozen at low temperatures. Thus, such a rapid increase of the specific heat may signal the onset of multifragmentation.

In order to explore the validity of this picture, we have performed a simple statistical calculation on the fragment yields. The system is assumed to appear as a configuration of distinct exitable nuclear fragments, $\{n_i\}$, where n_i is the multiplicity of the nuclear species i. The total partition function is then given by

$$\mathcal{Z} = \frac{1}{\mathcal{Z}_0} \sum_{\{n_i\}} \prod_i \frac{1}{n_i!} \mathcal{Z}_i^{n_i} \, {\rm e}^{-\beta V(\{n_i\})} \ , \qquad (57)$$

where $\mathcal{Z}_i$ is the contribution to partition function arising from a fragment of type i within the volume Ω,

$$\mathcal{Z}_i = \Omega \left(\frac{M_i T}{2\pi\hbar^2} \right)^{3/2} \zeta_i \ , \qquad (58)$$

and $\mathcal{Z}_0$ refers to the compound nucleus $^A Z$. The intrinsic degrees of freedom are taken into account through the effective intrinsic partition function ζ_i which contains the ground-state degeneracy $g_i = 2J_i^{g.s.} + 1$ and the excited levels up to $E^* = E_0 + \Delta \ (A_i - 4)$ for fragments with $A_i > 4$, where E_0 is the minimum energy for particle evaporation and $\Delta = 2$ MeV, as suggested in ref. [22]. Furthermore, the potential energy includes the binding energy difference and the inter-fragment Coulomb potential,

$$V(\{n_i\}) = B(A,Z) - \sum_\alpha B(A_\alpha, Z_\alpha) + \sum_{\alpha<\beta} V_{\alpha\beta} \ , \qquad (59)$$

where α and β enumerate the fragments in the particular configuration $\{n_i\}$. The fragment binding energies B are taken from experiment and the Coulomb interaction is fixed by the barrier height. Figure 4 shows the resulting the specific heat per nucleon calculated with this fragment canonical model with up to nine-fragment configurations included, as well as the *AMD* results from fig. 3 with $r_0 = 2.0$ fm. It is seen that the *AMD* behavior is well reproduced when a sufficient fragment multiplicity is admitted in the statistical calculation. It is especially noteworthy that the reproduction of the rapid increase at $T \sim 4$ MeV, requires the inclusion of channels with four or five fragments. This illustration shows that multifragmentation appears naturally as the volume is increased and, moreover, the model presented in this work can describe this phenomenon.

It is necessary to study statistical properties of heavier nuclei in order to fully elucidate the relation between multifragmentation and the liquid-gas phase transition,

since the latter is closely related to the properties of nuclear matter. Figure 5 shows the calculated excitation energy and specific heat for ^{40}Ca . Since the sampling number at each temperature and volume is only around 2×10^3, the statistical error is not small. However, the qualitative features are almost the same as for ^{12}C and, in particular, the low-temperature correspondence with the finite-temperature nuclear liquid-drop model is good.

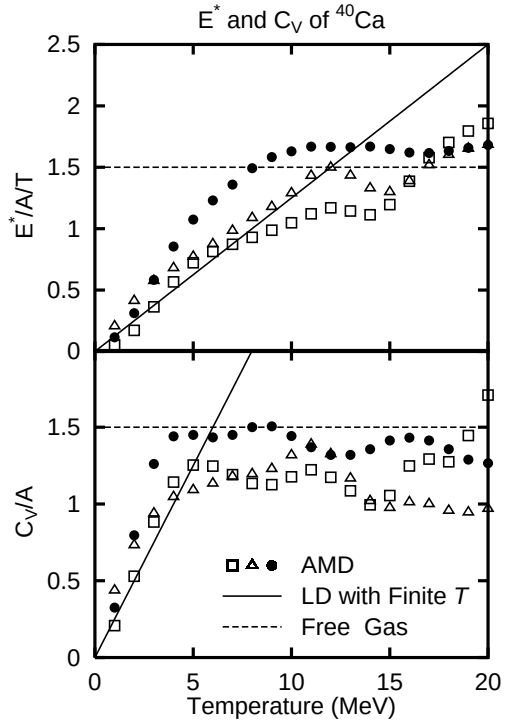

FIG. 5. Excitation energy and specific heat of ^{40}Ca.

The mean excitation energy per nucleon E^*/A divided by the temperature T (top) and the specific heat per particle C_V/A (bottom) for a canonical ensemble of ^{40}Ca nuclei calculated with the *AMD* model, in a display similar to fig. 3. The level-density parameter is $A/(8$ MeV).

4. DYNAMICS WITH QUANTAL FLUCTUATIONS

Until now we have studied the statistical properties of an assembly of nucleons. Below we briefly describe how the insights gained can be applied in dynamical scenarios. The most important result of the previous analyzes is that the quantal nature of the system demands that the energy dispersion of each wave packet be taken into account. This follows from the fact that the wave packet is not an eigenstate of the Hamiltonian operator and therefore the observed energy exhibits fluctuations around the given initial energy value [15]. This feature then affects the dynamical evolution significantly, as can be most easily seen from the expression for the microcanonical phase volume, as shown below. Since the long-time dynamical evolution of a closed system should reflect the associated microcanonical ensemble, we first discuss the statistical properties of a microcanonical ensemble.

4.1. Quantal microcanonical ensemble

For an ergodic system, in which each state is reachable from any given initial state, the long-time dynamical evolution should reflect the associated microcanonical ensemble. Therefore, the statistical properties of a dynamical model are related more closely to the microcanonical ensemble than to the canonical ensemble. The microcanonical phase volume is given by

$$\Omega(E) \equiv \mathrm{Tr}\left[\delta(\hat{H}-E)\right] = \int d\Gamma \; \frac{<\boldsymbol{Z}|\delta(\hat{H}-E)|\boldsymbol{Z}>}{<\boldsymbol{Z}|\boldsymbol{Z}>} = \int d\Gamma \; \rho_{_E}(\boldsymbol{Z}) \; . \tag{60}$$

Since the wave packets are not energy eigenstates, *i.e.* $\rho_{_E}(\boldsymbol{Z}) \neq \delta(\mathcal{H}-E)$, those states with $\mathcal{H} \neq E$ can also contribute to the microcanonical phase volume according to the probability of $\rho_{_E}(\boldsymbol{Z})$. It is interesting to note that resolution of unity (2) causes the strength function $\rho_{_E}(\boldsymbol{Z})$ plays a dual role: While it is defined as the energy distribution in a *single* wave packet $\boldsymbol{Z}$, it also expressed the relative weight of *different* wave packets in the microcanonical ensemble characterized by the energy E.

From the microcanonical phase volume (60), the ensemble temperature T can be defined unambiguously by means of the formal thermodynamical relation as the inverse of the rate at which the phase volume increases with energy,

$$\frac{1}{T} \equiv \frac{\partial}{\partial E} \; \log\Omega(E) = \frac{1}{\Omega(E)} \int \; d\Gamma \; \frac{\partial \rho_{_E}(\boldsymbol{Z})}{\partial E} = \frac{1}{\Omega(E)} \int \; d\Gamma \; \beta_{_E}(\boldsymbol{Z}) \; \rho_{_E}(\boldsymbol{Z}) \; , \tag{61}$$

where the contribution from a given wave packet is given by

$$\beta_{_E}(\boldsymbol{Z}) \equiv \frac{\partial}{\partial E} \; \log \rho_{_E}(\boldsymbol{Z}) \; . \tag{62}$$

We note that this latter state-dependent quantity can have either sign. (Since $\rho_{_E}(\boldsymbol{Z})$ is largest when $E \approx \mathcal{H}$, it will generally increase with E when $E < \mathcal{H}$ and decrease when $E > \mathcal{H}$.)

The microcanonical phase volume (60) is intimately related to the partition function of the associated canonical ensemble,

$$\mathcal{Z}(\beta) \equiv \int_0^\infty dE\ \Omega(E)\ \mathrm{e}^{-\beta E} = \int d\Gamma \int_0^\infty dE\ \rho_{_E}(\boldsymbol{Z})\mathrm{e}^{-\beta E}$$
$$= \int d\Gamma\ \mathcal{W}_\beta(\boldsymbol{Z})\ . \tag{63}$$

Thus statistical properties of both the microcanonical and the canonical ensemble can be studied on the same footing through $\rho_{_E}(\boldsymbol{Z})$ and $\mathcal{W}_\beta(\boldsymbol{Z})$. We also note that when the energy eigenvalue distribution of the given state $|\boldsymbol{Z}>$ is of Poisson form, we recover the same statistical weight $\mathcal{W}_\beta(\boldsymbol{Z})$ as found earlier (eq. (23)).

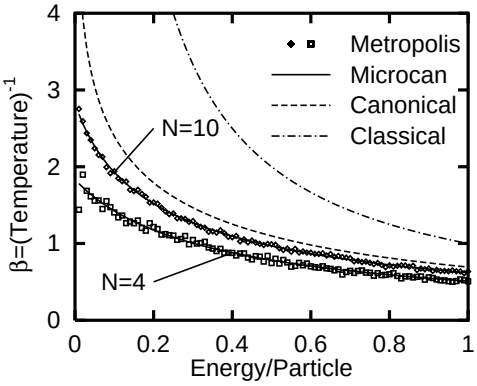

FIG. 6. Ensemble sampling of microcanonical temperature.

The inverse temperature of distinguishable particles in a harmonic oscillator as a function of the energy per particle, as obtained by performing a Metropolis sampling of the state dependent temperature (62) using the probability (64) for N =4 (squares) and 10 (diamonds) (10^4 states were sampled for each given energy). Also shown are the exact analytical results for the corresponding microcanonical (solid), canonical (dashed), and classical (dotted) ensembles.

In order to illustrate the situation, we consider a microcanonical ensemble of N distinguishable particles in a common harmonic oscillator and calculate the corresponding inverse ensemble temperature by means of eq. (61). The energy distribution $\rho_{_E}(\boldsymbol{Z})$ is assumed to be a continuous Poisson distribution,

$$\rho_{_E}(\boldsymbol{Z})\ \propto\ \mathrm{e}^{-\mathcal{H}}\ \frac{\mathcal{H}^E}{E!}\ =\ \mathrm{e}^{-\mathcal{H}}\ \frac{\mathcal{H}^E}{\Gamma(E+1)}\ , \tag{64}$$

using units in which $\hbar\omega = 1$. (The number of states for a given energy is then $\Omega(E) = \Gamma(E+N)/[\Gamma(E+1)\Gamma(N)]$.) Using the above expression as the weight function, it is then possible to employ the Metropolis sampling technique to calculate the average in eq. (61), $\prec \beta_E \succ$. The result is shown in fig. 6 and leads to a perfect reproduction of the exact inverse temperature for the microcanonical ensemble, as one should expect. The temperature depends on the number of particles N, even though the particles are distinguishable, and may be compared with the results for the corresponding canonical and classical ensembles.

4.2. Quantal Langevin force

It follows from the previous discussion that after the system has undergone a sufficiently long time evolution the probability distribution $\phi(\boldsymbol{Z})$ for finding the state $|\boldsymbol{Z}>$ should be proportional to the corresponding level density,

$$\phi(\boldsymbol{Z})\ \ \overset{t\to\infty}{\to}\ \ \rho_{_E}(\boldsymbol{Z}) = \mathrm{e}^{-\mathcal{F}(\boldsymbol{Z})}\ , \tag{65}$$

where

$$\mathcal{F} \equiv -\log \rho_{_E}(\boldsymbol{Z}) \tag{66}$$

plays the role of an effective potential for the parameter $\boldsymbol{Z}$. The evolution of the wave packet parameter vector, $\boldsymbol{Z}(t)$, as determined by the equation of motion (5), is entirely deterministic, without any physical effect of the spectral structure of the wave packet. Consequently, as we have discussed above, the system does not relax towards the appropriate quantum statistical equilibrium. Furthermore, this malady is inherent in the classical treatment and it could not be remedied by merely including a collision term in the standard manner, since the evolving wave packet would then still remain on the equi-Hamiltonian surface $\mathcal{H} = E$ and, therefore, the distribution $\phi(\boldsymbol{Z})$ would not relax to the microcanonical ensemble (65).

In order to provide the system with an opportunity for exploring and exploiting the various eigencomponents contributing to its wave packet, we wish to augment the equation of motion (5) by a stochastic term that may cause occasional transitions between different wave packets. The analogy of the distribution (65) with the classical Boltzmann distribution $\mathcal{W}_\beta(\boldsymbol{Z}) = \exp(-\beta\mathcal{H})$ suggests a way to introduce such a stochastic term, since the latter distribution can be obtained by introducing a Langevin term in the equation of motion. Analogously, the quantal distribution can be obtained by augmenting the deterministic equation of motion (5) by a Langevin term [23],

$$\dot{\boldsymbol{Z}}\ =\ \boldsymbol{h}\ +\ \boldsymbol{g}\cdot\boldsymbol{\zeta}\ , \tag{67}$$

where the dot over $\boldsymbol{Z}$ indicates the rate of change over and above that given by eq. (5) and the random complex vector $\boldsymbol{\zeta}$ represents white noise,

$$\prec \bar{\boldsymbol{\zeta}}_n(t)\ \boldsymbol{\zeta}_{n'}(t') \succ =\ 2\ \delta_{nn'}\ \delta(t-t')\ . \tag{68}$$

In order to see that the Langevin equation (67) indeed can produce the desired equilibrium distribution (65), it

is helpful to consider the corresponding Fokker-Planck equation,

$$\dot{\phi}(\boldsymbol{z}_1, \cdots, \boldsymbol{z}_A; t) = \left[-\sum_{n=1}^{A} \frac{\partial}{\partial \boldsymbol{z}_n} V_n + \sum_{nn'}^{A} \frac{\partial^2}{\partial \boldsymbol{z}_n \partial \bar{\boldsymbol{z}}_{n'}} M_{nn'} + \text{c.c.} \right] \phi \ , \quad (69)$$

The transport coefficients $\boldsymbol{V}$ and $\boldsymbol{M}$ govern the early growth rate of the average value of the parameter vector and the associated covariance tensor, respectively, starting from a given value $\boldsymbol{Z}$. Therefore, the diffusion coefficient is given by $\boldsymbol{M} = \boldsymbol{g} \cdot \boldsymbol{g}$. Furthermore, if we demand that the quantal distribution (65), $\phi \sim \exp(-\mathcal{F})$, be an equilibrium solution to this equation, the form of the drift coefficient follows,

$$V_n \ = \ -\sum_{n'} M_{nn'} \frac{\partial \mathcal{F}}{\partial \bar{\boldsymbol{z}}_{n'}} \ + \ \sum_{n'} \frac{\partial}{\partial \bar{\boldsymbol{z}}_{n'}} M_{nn'} \ . \quad (70)$$

The second term represents the noise-induced drift which enters in the general case when the tensor $\boldsymbol{M}$ depends on $\boldsymbol{Z}$ [23]. Since this dependence is often unimportant, we shall ignore this term in the following, for convenience.

Since $\mathcal{F}$ is predominantly determined by $\mathcal{H}$, its derivative is proportional to the driving force $\partial \mathcal{H} / \partial \bar{\boldsymbol{Z}}$ and the drift coefficient can then be rewritten,

$$\boldsymbol{V} \ \approx \ -\boldsymbol{M} \cdot \frac{\partial \mathcal{F}}{\partial \bar{\boldsymbol{Z}}} \ \approx \ -\beta_{\mathcal{H}} \ \boldsymbol{M} \cdot \frac{\partial \mathcal{H}}{\partial \bar{\boldsymbol{Z}}} \ . \quad (71)$$

We have here introduced the inverse state-dependent canonical temperature,

$$\beta_{\mathcal{H}}(\boldsymbol{Z}) \ \equiv \ \frac{\partial \mathcal{F}}{\partial \mathcal{H}} \ , \quad (72)$$

and the relation (71) is recognized as a manifestation of the Einstein relation.

The two state-dependent temperatures introduced, $\beta_E \equiv -\partial \mathcal{F} / \partial E$ and $\beta_{\mathcal{H}} \equiv \partial \mathcal{F} / \partial \mathcal{H}$, are identical if $\rho_{E}(\boldsymbol{Z})$ depends on E and $\boldsymbol{Z}$ only through either $\mathcal{H} - E$ or $\mathcal{H}/E$. This is approximately the case in most cases of interest and they can therefore be regarded as being very similar. For example, for the distinguishable particles considered in sect. 4 4.1, with the strength function given by (64), we have

$$\beta_{\mathcal{H}} = \frac{\mathcal{H} - E}{\mathcal{H}} \ , \quad (73)$$

$$\beta_{E} = \log(\mathcal{H}) - \frac{d}{dE} \log \Gamma(E+1) \ \approx \ \log(\mathcal{H}/E) = \beta_{\mathcal{H}} + \frac{1}{2} \beta_{\mathcal{H}}^2 + \cdots \ . \quad (74)$$

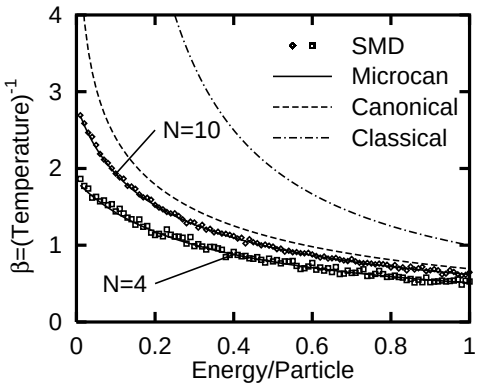

FIG. 7. Temporal sampling of microcanonical temperature.

The inverse temperature of distinguishable particles in a harmonic oscillator as a function of the energy per particle, as obtained by performing a sampling over the stochastic time evolution of a single initial state. The systems considered and the display are the same as in fig. 6 and 10^4 states were sampled for each given energy as well.

In order to illustrate the utility of the stochastic treatment, we show in fig. 7 the inverse ensemble temperature as obtained with the proposed Langevin equation (67). The systems are the same as those considered in fig. 6 and the integral over states is calculated by averaging over the configurations obtained at 10^4 time steps, starting from a single random initial wave packet. The results demonstrate that the quantal microcanonical distribution can be realized as a result of the stochastic pseudodynamics produced by eq. (67). This fact can be also seen from the resulting distribution of energy expectation values $P(\mathcal{H})$, as is illustrated in fig. 8 for N=10. Since the probability for finding the system with a given value of $\boldsymbol{Z}$ is proportional to $\rho_{E}(\boldsymbol{Z})$, the Hamiltonian distribution should be given by

$$P(\mathcal{H}) \ d\mathcal{H} = \ \rho_{E}(\boldsymbol{Z}) \ \frac{d\Gamma}{d\mathcal{H}} \ d\mathcal{H} \ \sim \ \rho_{E}(\boldsymbol{Z}) \ \mathcal{H}^{N-1} \ d\mathcal{H} \ . \quad (75)$$

The results indicate that this is indeed the case.

Although the stochastic term appearing here is somewhat similar to the usual random force that arises from the interaction between the particles under consideration and the heat bath in which they are embedded, it is important to recognize that the present random force arises from the energy dispersion of each wave packet and thus has a purely quantal origin. Therefore, we refer to this random force as the *quantal Langevin force*. We show below how this quantal Langevin force can be implemented once the interaction between the particles has been specified.

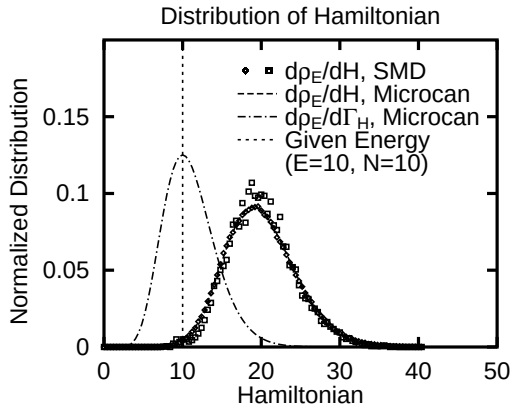

FIG. 8. Microcanonical distribution of the Hamiltonian.

The distribution of the expectation value of Hamiltonian operator, $\mathcal{H}$, for the systems considered in fig. 7, for the case with N=10 particles, based on samples of either 10^4 (squares) or 3×10^5 (diamonds) consequtive states generated by the proposed stochastic dynamics. Also shown are the result for the corresponding microcanonical ensembles (dashed curve) and that obtained without the phase-space factor $\mathcal{H}^{N-1}$ (dotted curve).

4.3. Characterization of the quantal Langevin force

In the preceding, we have introduced the Langevin equation and shown that it leads to the desired quantal equilibrium distribution. However, in order to apply the treatment to actual dynamical processes, it is necessary to determine the specific properties of the transport coefficients. For this purpose, we seek guidance from Fermi's golden rule and assume that the differential rate of transitions from a given wave packet $|\boldsymbol{Z}>$ to others near $|\boldsymbol{Z}'>$ is of the following form,

$$w(\boldsymbol{Z}\to\boldsymbol{Z}') \;=\; \frac{2\pi}{\hbar}\;|<\boldsymbol{Z}'_{_E}|\hat{V}|\boldsymbol{Z}_{_E}>|^2\;\rho_{_E}(\boldsymbol{Z}')\;. \quad (76)$$

Here the operator $\hat{V}$ represents a suitable "residual" interaction and E is a specified energy which is usually taken as the expectation value of the originally specified initial state. The utility of the above form (76) is underscored by the fact that it leads to the correct microcanonical equilibrium distribution. This can be verified by considering the equilibrium condition,

$$\phi(\boldsymbol{Z})\;w(\boldsymbol{Z}\to\boldsymbol{Z}')=\phi(\boldsymbol{Z}')\;w(\boldsymbol{Z}'\to\boldsymbol{Z})\;, \quad (77)$$

which is evidently satisfied when $\phi(\boldsymbol{Z})\sim\rho_E(\boldsymbol{Z})$, due to the symmetry of the matrix element in (76).

In analogy with the distortion occurring for the wave packets in a canonical ensemble (see sect. 2)), the initial and final states appearing in the above matrix element, $|\boldsymbol{Z}_{_E}>$ and $|\boldsymbol{Z}'_{_E}>$, are related to the actual states, $|\boldsymbol{Z}>$ and $|\boldsymbol{Z}'>$, by an appropriate distortion arising from the microcanonical constraint on the dynamical system. In principle, they should be the respective components of the wave packets associated with the energy eigenvalue E. However, since the projection to energy eigenstates poses a hard task, we have adopted the canonical distortion as a suitable approximation,

$$|\boldsymbol{Z}_{_E}>\approx\;\frac{|\boldsymbol{Z}(\beta_{\mathcal{H}}/2)>}{\sqrt{\mathcal{W}_\beta(\boldsymbol{Z})}}\;=\;\frac{\mathrm{e}^{-\beta_{\mathcal{H}}\hat{H}/2}|\boldsymbol{Z}>}{\sqrt{<\boldsymbol{Z}|\mathrm{e}^{-\beta_{\mathcal{H}}\hat{H}}|\boldsymbol{Z}>}}\;. \quad (78)$$

Application of the cooling equation (52) then yields the parameter characterizing the distorted wave packet,

$$\boldsymbol{Z}_{_E}=\boldsymbol{Z}+\frac{1}{2}\beta_{\mathcal{H}}\;\boldsymbol{F}\;. \quad (79)$$

It is easily seen that the energy expectation value of the distorted wave packet $|\boldsymbol{Z}_E>$ is equal to E, through first order in $\beta_{\mathcal{H}}$.

Simple approximate expressions for the moments of $w(\boldsymbol{Z}\to\boldsymbol{Z}')$ can be derived by expanding the transition rate (76) around $\boldsymbol{Z}_{_E}$, where both the matrix element and the energy spectrum have the largest values (see Appendix A). Then the transition rate from $\boldsymbol{Z}$ to a specific final state $\boldsymbol{Z}'$ is given by

$$\begin{aligned} w(\boldsymbol{Z}\to\boldsymbol{Z}') \;&\approx\; \frac{2\pi}{\hbar}|\mathcal{V}|^2\;\rho_{_E}(\boldsymbol{Z}_{_E}) \\ &\quad\times\mathrm{e}^{-(\delta\bar{\boldsymbol{Z}}-\frac{1}{2}\beta_{\mathcal{H}}\bar{\boldsymbol{F}})\cdot\boldsymbol{C}\cdot(\delta\boldsymbol{Z}-\frac{1}{2}\beta_{\mathcal{H}}\boldsymbol{F})}\;, \end{aligned} \quad (80)$$

where $\delta\boldsymbol{Z}=\boldsymbol{Z}'-\boldsymbol{Z}$ and $\mathcal{V}\equiv<\boldsymbol{Z}_{_E}|\hat{V}|\boldsymbol{Z}_{_E}>$ denotes the expectation value of the interaction in the initial state $\boldsymbol{Z}$. The total rate of transitions from the given state $\boldsymbol{Z}$ into any final state $\boldsymbol{Z}'$ can now be readily calculated,

$$w_0(\boldsymbol{Z})\;\equiv\;\int d\Gamma'\;w(\boldsymbol{Z}\to\boldsymbol{Z}')\;\approx\;\frac{2\pi}{\hbar}\;|\mathcal{V}|^2\rho_{_E}(\boldsymbol{Z}_{_E})\;. \quad (81)$$

The expected number of transitions taking place during a small time interval Δt is then $n_0=w_0\Delta t$, which may also be interpreted as the probability that a transition occurs during Δt. Therefore this total rate w_0 can be regarded as the inverse lifetime of the wave packet $|\boldsymbol{Z}>$.

Since the transport coefficients $\boldsymbol{V}$ and $\boldsymbol{M}$ govern the early growth rate of the average value of the parameter vector $\boldsymbol{Z}$ and the associated covariance tensor, respectively, they can be obtained from the moments of the microscopic transition rate,

$$\begin{aligned} V_n\;&\equiv\;\int d\Gamma'\;\delta\boldsymbol{z}_n\;w(\boldsymbol{Z}\to\boldsymbol{Z}') \\ &\approx\;-w_0\beta_{\mathcal{H}}\left(\boldsymbol{C}^{-1}\cdot\frac{\partial\mathcal{H}}{\partial\bar{\boldsymbol{Z}}}\right)_n=w_0\beta_{\mathcal{H}}\boldsymbol{F}\;, \end{aligned} \quad (82)$$

$$M_{nn'}\;\equiv\;\int d\Gamma'\;\delta\boldsymbol{z}_n\;\delta\bar{\boldsymbol{z}}_{n'}\;w(\boldsymbol{Z}\to\boldsymbol{Z}') \quad (83)$$

$$\approx\;w_0\;(\boldsymbol{C}^{-1})_{nn'}\;, \quad (84)$$

to leading order in $\beta_{\mathcal{H}}$. We note that the Einstein relation (71) is indeed satisfied by these expressions and, moreover, the drift coefficient is proportional to the generalized force $\boldsymbol{F}$, as would be expected. It may also be remarked that both the center-of-mass position and the total momentum remain unchanged on the average, since $\sum_n V_n = 0$, while the individual dynamical evolutions will exhibit diffusive Brownian-type excursions around those averages. This behavior is to be expected, since the the energy $\mathcal{H}$ is no longer a constant of motion but will fluctuate around the specified value E.

The above simple approximate expressions (81), (82), and (84) make it possible to simulate the Langevin evolution by picking the stochastic changes $\delta \boldsymbol{z}_n$ in accordance with the transport coefficients $\boldsymbol{V}$ and $\boldsymbol{M}$. It is here important that the overlap matrix $\boldsymbol{C}$ is positive definite so its square root exists. Thus it is fairly straightforward to implement the proposed stochastic treatment.

5. SUMMARY

In the present work, we have addressed the treatment of quantum fluctuations in microscopic descriptions based on wave packets, a problem encountered in a broad range of fields involving quantum physics. Since the wave packets are not energy eigenstates, the statistical operator $\exp(-\beta\hat{H})$ cannot be treated as a c-number. In order to take account of the associated spectral distribution and ensure that the statistical properties are quantal, it is necessary to introduce suitable modifications relative to the ordinary equations of motion for the wave packet parameters which are basically classical in character, having been derived from the time-dependent variational principle.

We have formulated a simple but apparently successful treatment by including the first correction term in the cumulant expansion of the statistical weight. The associated small parameter is $\sigma_E^2/T\mathcal{H}$, where $\mathcal{H} \equiv < \boldsymbol{Z}|\hat{H}|\boldsymbol{Z} >$ is the mean energy of a wave packet and σ_E^2 is the corresponding energy variance. This approach is exact when the spectral distribution is of Poisson form, as is often the case (at least approximately), and the corresponding effective level spacing is $D \equiv -\partial \log \mathcal{H}_\beta/\partial\beta = \sigma_E^2/\mathcal{H}$. It is then straightforward to write down the improved expression for the statistical weight. Moreover, the associated thermal distortion of the internal structure of the wave packet was determined.

Since our initial suggestion [11] that this treatment might be useful has led to some debate [13,14], we discussed and illustrated the various possible approaches to determining the statistical behavior of one-body observables, such as the occupation number. In this manner, it was brought out that although it is possible to recover the quantal appearance of single-particle observables by suitable redefinition of the temperature parameter, such attempts do not yield the proper many-body properties, as governed by the behavior of the partition function. The key to resolving the issue lies in the inevitable distortion of the wave packet caused by the canonical operator $\exp(-\beta\hat{H})$.

To illustrate the practical utility of the treatment, we considered the statistical properties of finite nuclei, as exemplified by ^{12}C and ^{40}Ca. The low-temperature behavior matches well with the finite-temperature liquid-drop model. Moreover, as the temperature is raised, that the nuclear liquid drop evolves into a fragment gas, as is expected for actual nuclar systems and in good agreement with the standard statistical multifragmentation model.

We then turned to the important issue of how to incorporate the quantum fluctuations into the dynamics. Here the key suggestion is to allow the system to explore its spectral distribution by introducing suitable stochastic transitions between the wave packets [15]. This can conveniently be done by means of a Langevin term in the equations of motion for the wave packet parameters. We derived the general form of the associated transport coefficients and verified that the proper microcanonical equilibrium distribution is indeed achieved. Simple approximate expressions for the specific values of the transport coefficients were then obtained by means of Fermi's golden rule, leading to a practically useful treatment. It is important to recognize that although the Langevin term may resemble the effect of the standard collision term, its origin is different: While the former results from the residual interaction, the latter arises from the quantum fluctuations that are inherent in the wave packets employed in the description.

The proposed extension of the standard treatment represents a formally well based approach towards incorporating the effect of quantum fluctuations into the wave packet dynamics. Moreover, it leads to the desired statistical properties in static scenarios and can be included in the dynamics in a conceptually simple and tractable manner. The method may therefore find useful application in the context of microscopic simulations of actual many-body processes, such as fragment production in heavy-ion collisions.

This work was supported in part by the Grant-in-Aid for Scientific Research (No. 06740193) from the Ministry of Education, Science and Culture, Japan, and by the Director, Office of Energy Research, Office of High Energy and Nuclear Physics, Nuclear Physics Division of the U.S. Department of Energy under Contract No. DE-AC03-76SF00098. One of the authors (A.O.) also thanks the Ministry of Education, Science and Culture, Japan, for the Overseas Research Fellowship to him. The calculations in this work were supported by Research Center for Nuclear Physics (RCNP), Osaka University, as RCNP Computational Nuclear Physics Project No. 93-B-03.

APPENDIX A: MOMENTS OF THE TRANSITION RATE

In this appendix, we show some technical details regarding the calculation of the transition rate and its first and second moments which are required in sect. 4 4.3.

We start by rewriting the matrix element in the transition rate (76),

$$| < \boldsymbol{Z}'|\hat{V}|\boldsymbol{Z} > |^2 = \mathcal{V}(\bar{\boldsymbol{Z}}', \boldsymbol{Z})\ \mathcal{V}(\bar{\boldsymbol{Z}}, \boldsymbol{Z}')\ | < \boldsymbol{Z}'|\boldsymbol{Z} > |^2\ , \tag{A1}$$

where $\mathcal{V}(\bar{\boldsymbol{Z}}', \boldsymbol{Z}) \equiv (\boldsymbol{Z}'|\hat{V}|\boldsymbol{Z})/(\boldsymbol{Z}'|\boldsymbol{Z})$. The overlap between two normalized states is approximately of Gaussian form,

$$| < \boldsymbol{Z}'|\boldsymbol{Z} > |^2 \ \approx\ \exp\left(-\delta\bar{\boldsymbol{Z}} \cdot \boldsymbol{C} \cdot \delta\boldsymbol{Z}\right)\ , \tag{A2}$$

as can be seen by expanding in $\delta\boldsymbol{Z} = \boldsymbol{Z}' - \boldsymbol{Z}$,

$$\log | < \boldsymbol{Z}'|\boldsymbol{Z} > |^2 \ =\ -\delta\bar{\boldsymbol{Z}} \cdot \boldsymbol{C} \cdot \delta\boldsymbol{Z}\ +\ \mathcal{O}\left((\delta\boldsymbol{z})^3\right)\ . \tag{A3}$$

The above expression (A2) is consistent with the fact that $d\bar{\boldsymbol{Z}} \cdot \boldsymbol{C} \cdot d\boldsymbol{Z}$ defines a infinitesimal squared distance between two wave packets and, accordingly, that $\det \boldsymbol{C}$ appears in the canonical measure. Furthermore, the relation is exact when $\boldsymbol{C}$ is unity, *i.e.* when antisymmetrization is ignored.

Using the expression (A2) and assuming that $\boldsymbol{Z}'_{_E}$ is close to $\boldsymbol{Z}_{_E}$, we obtain

$$| < \boldsymbol{Z}'_{_E}|\hat{V}|\boldsymbol{Z}_{_E} > |^2 \tag{A4}$$

$$\approx\ \left|\mathcal{V}(\bar{\boldsymbol{Z}}_{_E}, \boldsymbol{Z}_{_E})\right|^2\ \mathrm{e}^{-\left(\bar{\boldsymbol{Z}}'_{_E} - \bar{\boldsymbol{Z}}_{_E}\right)\cdot\boldsymbol{C}\cdot\left(\boldsymbol{Z}'_{_E} - \boldsymbol{Z}_{_E}\right)}\ . \tag{A5}$$

Finally, when $\boldsymbol{Z}'_{_E} \approx \boldsymbol{Z}_{_E}$ then $\beta_{\mathcal{H}'}$ is small and the distortion can be ignored, $\boldsymbol{Z}' \approx \boldsymbol{Z}'_{_E}$. Thus we arrive at the total transition rate given in eq. (81).

We have used the resolution of unity,

$$\int d\Gamma'\ < \boldsymbol{Z}|\boldsymbol{Z}' > < \boldsymbol{Z}'|\boldsymbol{Z} > \ =\ \int d\Gamma'\ \mathrm{e}^{-\delta\bar{\boldsymbol{Z}}\cdot\boldsymbol{C}\cdot\delta\boldsymbol{Z}} = 1\ , \tag{A6}$$

and the first and second moment can be calculated by invoking the formulas

$$\int d\Gamma'\ \delta\boldsymbol{z}_n \exp\left(\delta\bar{\boldsymbol{Z}} \cdot \boldsymbol{C} \cdot \delta\boldsymbol{Z}\right) = 0\ , \tag{A7}$$

$$\int d\Gamma'\ \delta\boldsymbol{z}_n \delta\bar{\boldsymbol{z}}_{n'} \exp\left(\delta\bar{\boldsymbol{Z}} \cdot \boldsymbol{C} \cdot \delta\boldsymbol{Z}\right) = (C^{-1})_{nn'}\ . \tag{A8}$$

In our previous work [15], we have subtracted the self-transition matrix element and expanded $\mathcal{V}$ in $\delta\boldsymbol{Z}$. While this subtraction reduces the total transition rate, the relation between the drift and diffusion coefficients (71) remains valid.

[1] P. Kreutz et al., Nucl. Phys. **A556** (1993), 672.
[2] K. Hagel et al., Phys. Rev. Lett. **68** (1992), 2141.
[3] M.B. Tsang et al., Phys. Rev. Lett. **71** (1993), 1502.
[4] G.F. Bertsch and S. Das Gupta, Phys. Rep. **160** (1988), 189; W. Cassing, V. Metag, U. Mosel, and K. Niita, Phys. Rep. **188** (1990), 363.
[5] J. Aichelin and H. Stöcker, Phys. Lett. **B176** (1986), 14; J. Aichelin, Phys. Rep. **202** (1991), 233; G. Peilert H. Stöcker, W. Greiner, A. Rosenhauer, A. Bohnet, and J. Aichelin, Phys. Rev. **C39** (1989), 1402.
[6] Toshiki Maruyama, A. Ohnishi, and H. Horiuchi, Phys. Rev. **C42** (1990), 386; Phys. Rev. **C45** (1992), 2355; Toshiki Maruyama, A. Ono, A. Ohnishi, and H. Horiuchi, Prog. Theor. Phys. **87** (1992), 1367.
[7] D.H. Boal and J.N. Glosli, Phys. Rev. **C38** (1988), 2621.
[8] A. Ono, H. Horiuchi, Toshiki Maruyama, and A. Ohnishi, Phys. Rev. Lett. **68** (1992), 2898: Prog. Theor. Phys. **87** (1992), 1185; Phys. Rev. **C47** (1993), 2652.
[9] A. Ono, H. Horiuchi, and Toshiki Maruyama, Phys. Rev **C48** (1993), 2946; A. Ono and H. Horiuchi, Phys. Rev. **C51** (1995), 299; E.I. Tanaka, A. Ono, H. Horiuchi, Tomoyuki Maruyama, and A. Engel, Phys. Rev. **C52** (1995), 316; A. Engel, E. I. Tanaka, Tomoyuki Maruyama, A. Ono, and H. Horiuchi, Phys. Rev. **C** (1995), to be published.
[10] H. Feldmeier, Nucl. Phys. **A515** (1990), 147; H. Feldmeier, K. Bieler, and J. Schnack, Nucl. Phys. **A586** (1995), 493; H. Feldmeier and J. Schnack, Nucl. Phys. **A583** (1995), 347.
[11] A. Ohnishi and J. Randrup, Nucl. Phys. **A565** (1993), 474.
[12] A. Ono, private communication, 1992.
[13] J. Schnack and H. Feldmeier, preprint, GSI-95-34, 1995.
[14] A. Ono and H. Horiuchi, preprint, RIKEN-AF-NP-214, 1995.
[15] A. Ohnishi and J. Randrup, Phys. Rev. Lett. **75** (1995), 596.
[16] Y. Abe, C. Gregoire, and H. Delagrange, J. Physique **47** (1986), C4-329; T. Wada, Y. Abe and N. Carjan, Phys. Rev. Lett. **70** (1993), 3538.
[17] J. Randrup and B. Remaud, Nucl. Phys. **A514** (1990), 339; G.F. Burgio, Ph. Chomaz, and J. Randrup, Nucl. Phys. **A529** (1991), 157; F. Chapelle, G.F. Burgio, Ph. Chomaz, and J. Randrup, Nucl. Phys. **A540** (1992), 227.
[18] S. Ayik and C. Gregoire, Phys. Lett. **B212** (1988), 269; Nucl. Phys. **A513** (1990), 187.
[19] F.S. Zhang and E. Suraud, Phys. Lett. **B319** (1993), 35.
[20] A. Volkov, Nucl. Phys. **75** (1965), 33.
[21] D. H. E. Gross, Rep. Prog. Phys. **53** (1990), 605, Nucl. Phys. **A553** (1993), 175c; X.-Z. Zhang, et al., Nucl. Phys. **A461** (1987), 641, 668.
[22] G. Fai and J. Randrup, Nucl. Phys. **A381** (1982), 557.
[23] Risken, *The Fokker-Planck Equation*, Springer (New York, 1989).